



RESEARCH ACTIVITIES

Theoretical and Computational Molecular Science

It is our goal to develop new theoretical and computational methods based on quantum mechanics, statistical mechanics, and molecular simulation in order to predict and understand the structures, reactions, and functions of molecules in gas, solution, and condensed phases as well as in nano- and bio-systems prior to or in cooperation with experiments.

Theoretical Study and Design of Functional Molecules: New Bonding, Structures, and Reactions

Department of Theoretical and Computational Molecular Science
Division of Theoretical Molecular Science I



NAGASE, Shigeru	Professor (–March, 2012)*
LUO, Gangfu	IMS Fellow†
KATOUDA, Michio	Post-Doctoral Fellow‡
GUO, Jing-Doing	Post-Doctoral Fellow*
KARTHIKEYAN, Subramanlan	Post-Doctoral Fellow§
ZHOU, Xin	Post-Doctoral Fellow
SAKAKI, Shigeyoshi	Visiting Scientist*
YAMADA, Mariko	Secretary
KONDO, Naoko	Secretary

In theoretical and computational chemistry, it is an important goal to develop functional molecules prior to or in cooperation with experiment. Thus, new bonds and structures provided by heavier atoms are investigated together with the reactivities. In addition, chemical modification and properties of nano-carbons are investigated to develop functional nanomolecular systems. Efficient computational methods are also developed to perform reliable quantum chemistry calculations for small and large molecular systems.

1. Quest for Stable Multiple Bonds between Lead Atoms

The heavier analogues of alkynes, REER (E = Si, Ge, Sn, Pb), have attracted special interest in main-group element chemistry. Accordingly, all the heavier analogues have been synthesized and isolated up to now. The X-ray crystal structure of the heaviest analogue, Ar*PbPbAr* (Ar* = C₆H₃-2,6-(C₆H₂-2,4,6-*i*-Pr₃)₂), has shown that the Pb–Pb bond distance is much longer than Pb–Pb single bond distances. Theoretical calculations have revealed that Ar*PbPbAr* has no π bond between Pb atoms. Therefore, it has been widely accepted that the heaviest Pb analogues of alkynes take a singly bonded structure, unlike the Si, Ge, and Sn cases. However, we have pointed out that Ar*PbPbAr* has a triply bonded structure in solution and crystal structures are not very helpful for compounds with bulky groups.¹⁾

The Pb–Pb bond distance of 3.071 Å calculated for the triply bonded structure of Ar*Pb–PbAr* is considerably longer than the Pb–Pb single bond distance of 2.844 Å in Ph₃PbPbPh₃. Since we have found that electropositive silyl groups decreases the Pb–Pb bond distance, several bulky silyl groups were tested using density functional calculations.²⁾ The optimized structure of R^{Si}PbPbR^{Si} (R^{Si} = SiⁱPr{CH(SiMe₃)₂}₂) is depicted in Figure 1, the two Pb atoms being triply bonded. The Pb–Pb bond distance of 2.696 Å is remarkably shorter

than the Pb–Pb single bond distance of 2.844 Å in Ph₃Pb–PbPh₃, and it is considerably shorter than the shortest Pb–Pb double bond distance of 2.903 Å known to date. However, the triply bonded structure is 4.3 kcal/mol less stable than the singly bonded structure. We are still searching for good substituent groups that stabilize a triply bonded structure with a sufficiently short Pb–Pb bond.

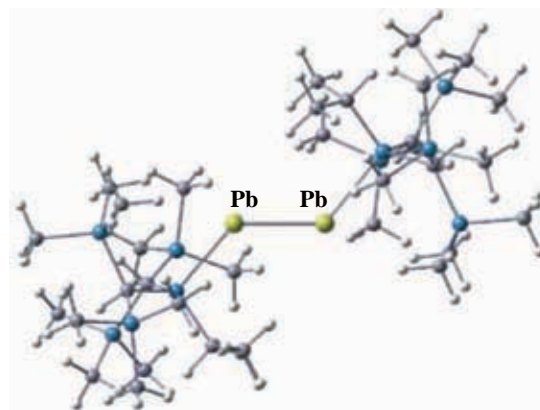


Figure 1. Triply bonded structure of R^{Si}PbPbR^{Si}.

As a new type of double bonds, diatomic molecules stabilized by the coordination of dative N-heterocyclic carbenes are of considerable interest currently. This stabilization has been performed for the synthesis and isolation of L:→Si=Si←:L and L:→Ge=Ge←:L (L = :C[N(2,6-*i*-Pr₂-C₆H₃)CH]₂). The Si–Si and Ge–Ge bond distances compare well with typical double bond distances of R₂Si=SiR₂ and R₂Ge=GeR₂. Because the heaviest Pb case remains unknown, we have investigated L:→Pb=Pb←:L.²⁾ The optimized structure is shown in Figure 2. Molecular orbital analysis confirms that the two Pb atoms are doubly bonded. It is notable that the Pb–Pb double bond distance of 2.833 Å is considerably shorter than the shortest Pb–Pb double bond distance of 2.903 Å known to date and

differs little from the Pb–Pb bond distance of Pb₂. It is expected that L:→Pb=Pb←:L is an interesting synthetic target.

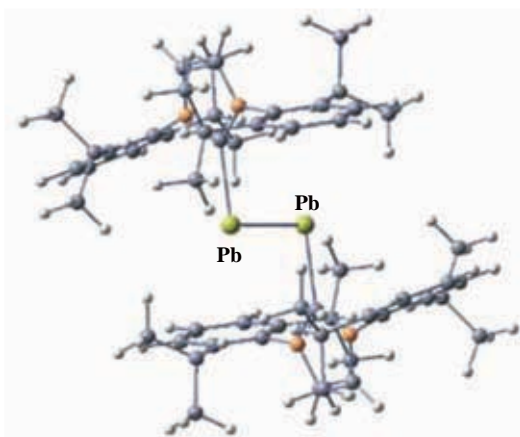
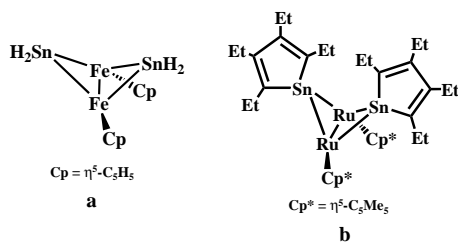


Figure 2. Optimized structure of L:→Pb=Pb←:L.

2. Short Bonds between Transition Metals

As a novel transition metal complex with an unsupported two-coordinate Fe atom, R*FeFe(η⁵-C₅H₅)(CO)₂ (R* = C₆H-2,6-Ar₂-3,5-ⁱPr₂ where Ar = C₆H₂-2,5,6-ⁱPr₃) has recently been synthesized and investigated.³⁾ X-ray crystal analysis shows that the Fe–Fe bond distances of 2.393 Å is much shorter than the known unsupported Fe–Fe bond distances (2.687–3.138 Å), suggesting that R*FeFe(η⁵-C₅H₅)(CO)₂ has the shortest unsupported Fe–Fe bond. Interestingly, calculations show that the Fe–Fe bond is greatly shortened in the bicyclic four-membered ring presented in Figure 3a.²⁾

Figure 3. Bicyclic four-membered ring complexes.



It is remarkable that the Fe–Fe bond distance of 2.045 Å is much shorter than the shortest Fe–Fe bond distance of 2.127 Å reported to date. This bond shortening assisted by two Sn atoms is very recently realized for the bicyclic four-membered Ru₂Sn₂ ring complex presented in Figure 3b.⁴⁾ The Ru–Ru bond distance of 2.343 Å determined through X-ray crystal analysis agrees well with the calculated value of 2.363 Å. It is shorter than the Ru–Ru distance of 2.449–2.469 Å in the

related bridge complexes, for which it is assumed that the two Ru atoms are triply bonded. Localized molecular orbital analysis reveals that one clear σ bond exists between the Ru atoms, while two three-centered σ orbitals are delocalized over each of the three-membered Ru₂Sn rings, which make an important contribution to Ru–Ru bonding. As a result, the Ru–Ru bond has a somewhat multiple-bond character.

It is also predicted theoretically that the Ru–Ru bond distance in the bicyclic four-membered Ru₂Sn₂ ring is shortened further in the bicyclic six-membered Ru₂Sn₄ ring. Experimental confirmation is in progress.

3. Nano-Carbon Systems

We have performed theoretical calculations for (a) polarized nonresonant Raman spectra of graphene nanoribbons⁵⁾ and (b) transport properties of transition metal intercalated graphene.⁶⁾ In collaboration with experiment, we have also performed calculations for (c) stable radical anions inside fullerene cages,⁷⁾ (d) the core-shell interplay in carbide cluster metallofullerenes,⁸⁾ (e) the cocrystal of La@C₈₂ and nickel porphyrin with high electron mobility,⁹⁾ and (f) chemical understanding of carbide cluster metallofullerenes.¹⁰⁾

References

- 1) N. Takagi and S. Nagase, *Organometallics* **26**, 3627–3629 (2007).
- 2) S. Nagase, *Pure Appl. Chem.*, in press.
- 3) H. Lei, J. -D. Guo, J. C. Fettinger, S. Nagase and P. P. Power, *J. Am. Chem. Soc.* **132**, 17399–17401 (2010).
- 4) T. Kuwabara, M. Saito, J. -D. Guo and S. Nagase, to be submitted for publication.
- 5) G. Luo, L. Wang, H. Li, R. Qui, J. Zhou, L. Li, Z. Gao, W. -N. Mei, J. Lu and S. Nagase, *J. Phys. Chem. C* **115**, 24463–24468 (2011).
- 6) J. Zhou, L. Wang, R. Qin, J. Zheng, W. N. Mei, P. A. Dowben, S. Nagase, Z. Gao and J. Lu, *J. Phys. Chem. C* **115**, 25273–25280 (2011).
- 7) T. Tsuchiya, M. Wielopolski, N. Sakuma, N. Mizorogi, T. Akasaka, T. Kato, D. M. Guldi and S. Nagase, *J. Am. Chem. Soc.* **133**, 13280–13283 (2011).
- 8) H. Kurihara, X. Lu, Y. Iiduka, H. Nikawa, M. Hachiya, N. Mizorogi, Z. Slanina, T. Tsuchiya, S. Nagase and T. Akasaka, *Inorg. Chem.* **51**, 746–750 (2012).
- 9) S. Sato, H. Nikawa, S. Seki, L. Wang, G. Luo, J. Lu, M. Haranaka, T. Tsuchiya, S. Nagase and T. Akasaka, *Angew. Chem., Int. Ed.* **51**, 1589–1591 (2012).
- 10) H. Kurihara, X. Lu, Y. Iiduka, H. Nikawa, N. Mizorogi, Z. Slanina, T. Tsuchiya, S. Nagase and T. Akasaka, *J. Am. Chem. Soc.* **134**, 3139–3144 (2012).

* Present Address; Fukui Institute for Fundamental Chemistry, Kyoto University, Kyoto 606-8103

† Present Address; Department of Physics, Peking University, Beijing 100871, P. R. China

‡ Present Address; Riken Advanced Institute for Computational Science, Kobe 650-0047

§ Present Address; Department of Chemistry, Sungkyunkwan University, Suwon 440-746, Korea

|| Present Address; Harbin Institute of Technology, Harbin 150080, P. R. China

Electron and Electromagnetic Field Dynamics in Nanostructures

Department of Theoretical and Computational Molecular Science
Division of Theoretical Molecular Science I



NOBUSADA, Katsuyuki Associate Professor
YASUIKE, Tomokazu Assistant Professor
IIDA, Kenji IMS Fellow
NODA, Masashi Post-Doctoral Fellow
YAMADA, Mariko Secretary

We have developed theoretical methods to calculate photo-induced electron dynamics in nanostructured materials such as nanoparticles, quantum-dot arrays, and adsorbate-surface systems. Specifically, we have formulated generalized theory of a light-matter interaction beyond a dipole approximation with the aim of understanding the near-field excitation of nanostructures. Furthermore, a highly efficient computational program of massively parallel calculations for electron dynamics has been developed to investigate optical response of nanostructures more than ten-nanometers. Structural and electronic properties of gold-thiolate clusters have also been elucidated in collaboration with an experimental group.

1. Massively-Parallel TDDFT Calculations Based on Finite Difference Method in Real-Time and Real-Space

A highly efficient computational program of massively parallel calculations for electron dynamics has been developed in an effort to apply the method to optical response of nanostructures more than ten-nanometers. The approach is based on time-dependent density functional theory calculations in real-time and real-space. The computational code is implemented by using very simple algorithms with a finite difference method in space derivative and Taylor expansion in time-propagation. Since the computational program is free from the algorithms of eigenvalue problems and fast-fourier-transformation, which are usually implemented in conventional quantum chemistry or band structure calculations, the program is highly suitable for massively parallel calculations. The method is applied to optical response of nanostructures constructed from C_{60} as benchmark systems. We achieved 8.15% peak performance on the K computer with 1920 nodes (15360 cores) and 3.25% peak performance with 12288 nodes (98304 cores). The peak performance decreases with increasing the nodes because of the network communications due to summing up electron density. The computed absorption spectrum of a

face-centered cubic unit of solid C_{60} well reproduces the experimental result.

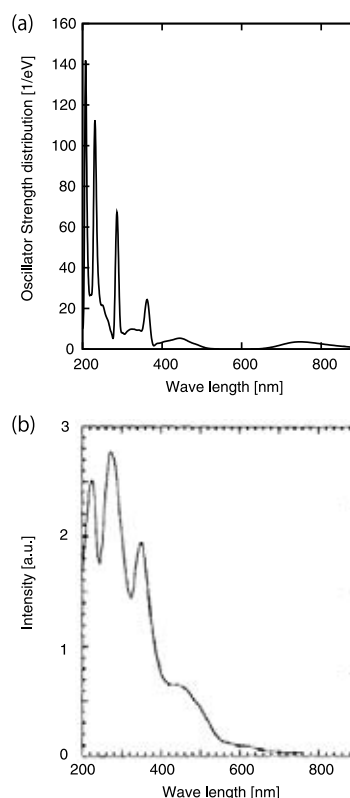


Figure 1. (a) Absorption spectrum of a face-centered cubic unit associated with a solid thin film of C_{60} in comparison with (b) the experimental observation.

2. Enhanced Raman Spectrum of Pyrazine with the Aid of Resonant Electron Dynamics in a Nearby Cluster¹⁾

We have investigated the electron dynamics relevant to the

Raman enhancement of pyrazine by a nearby Na_4 cluster. The present time-dependent analysis allows us to illustrate that the electronic excitation in Na_4 is closely associated with surface-enhanced Raman scattering in pyrazine. More specifically, it was clearly demonstrated that some specific enhanced vibrational modes strongly couple with the plasmonic electron motion of Na_4 . The displacement along the enhanced mode leads to a change of the electron dynamics in the entire region of the system, whereas the non-enhanced mode causes only a localized change in the junction area between pyrazine and Na_4 . The strong obstructive mode to the plasmonic electron motion is strongly enhanced. In the present system, all the obstructive modes are readily understood by the characteristics of the atoms in-phase oscillating in the x -direction at the side of Na_4 . This picture gives a clear explanation for the enhancement. The present results show the potential ability of cluster-enhanced Raman scattering. A microcluster selectively adsorbed by a specific molecule can be designed using recently developed techniques for the chemical synthesis of clusters. Such artificially designed clusters significantly enhance the Raman scattering of analyte molecules and therefore provide a new way of utilizing enhanced Raman scattering in various research fields.

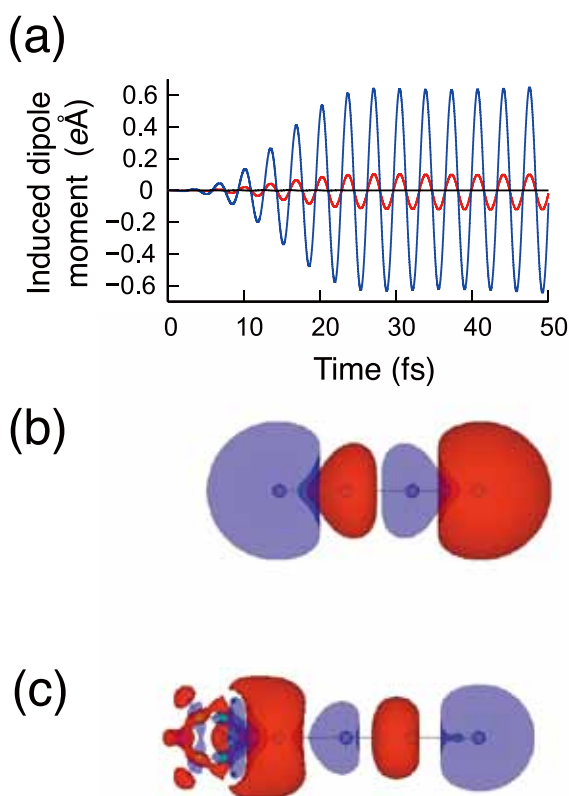


Figure 2. (a) Time-dependent induced dipole moments (x -component) in the $\text{C}_4\text{H}_4\text{N}_2$ (red) and Na_4 (blue) sides of $\text{C}_4\text{H}_4\text{N}_2\text{-Na}_4$ under x -polarized laser excitation at $\omega = 1.23$ eV. The dipole moment of isolated $\text{C}_4\text{H}_4\text{N}_2$ under the same excitation condition is also shown (black). Fourier component (1.23 eV) of the time-dependent induced density of (b) Na_4 and (c) $\text{C}_4\text{N}_2\text{H}_4\text{-Na}_4$.

3. Palladium Doping of Magic Gold Cluster $\text{Au}_{38}(\text{SC}_2\text{H}_4\text{Ph})_{24}$: Formation of $\text{Pd}_2\text{Au}_{36}(\text{SC}_2\text{H}_4\text{Ph})_{24}$ with Higher Stability than $\text{Au}_{38}(\text{SC}_2\text{H}_4\text{Ph})_{24}$ ²⁾

Gold clusters protected by thiolates have attracted considerable attention as building blocks for new functional materials because they exhibit size-specific physical and chemical properties. Among these, $\text{Au}_{25}(\text{SR})_{18}$, $\text{Au}_{38}(\text{SR})_{24}$, $\text{Au}_{68}(\text{SR})_{34}$, $\text{Au}_{102}(\text{SR})_{44}$, and $\text{Au}_{144}(\text{SR})_{60}$ are promising, because they exhibit higher thermodynamic and chemical stabilities than clusters of other sizes. Many studies have been conducted on the isolation, size-selective synthesis, stabilities, structures, chemical and physical properties, and applications of these stable clusters. In this study, a phenylethanethiolate-protected $\text{Pd}_2\text{Au}_{36}(\text{SC}_2\text{H}_4\text{Ph})_{24}$ cluster, which is a two-Pd atom-doped cluster of the well studied magic gold cluster $\text{Au}_{38}(\text{SC}_2\text{H}_4\text{Ph})_{24}$, was synthesized in high purity and its stability was investigated. The experimental and theoretical results demonstrate that $\text{Pd}_2\text{Au}_{36}(\text{SC}_2\text{H}_4\text{Ph})_{24}$ is more stable than $\text{Au}_{38}(\text{SC}_2\text{H}_4\text{Ph})_{24}$ against degradation in solution and core etching by thiols.

4. Effect of Copper Doping on Electronic Structure, Geometric Structure, and Stability of Thiolate-Protected Au_{25} Nanoclusters³⁾

Several recent studies have attempted to impart $[\text{Au}_{25}(\text{SR})_{18}]^-$ with new properties by doping with foreign atoms. In this study, we investigated the effect of copper doping on the electronic structure, geometric structure, and stability of $[\text{Au}_{25}(\text{SR})_{18}]^-$ with the aim of investigating the effect of foreign atom doping of $[\text{Au}_{25}(\text{SR})_{18}]^-$. $\text{Cu}_n\text{Au}_{25-n}(\text{SC}_2\text{H}_4\text{Ph})_{18}$ was synthesized by reducing complexes formed by the reaction between metal salts (copper and gold salts) and $\text{PhC}_2\text{H}_4\text{SH}$ with NaBH_4 . Mass analysis revealed that the products contained $\text{Cu}_n\text{Au}_{25-n}(\text{SC}_2\text{H}_4\text{Ph})_{18}$ ($n = 1\text{--}5$) in high purity. Experimental and theoretical analysis of the synthesized clusters revealed that copper doping alters the optical properties and redox potentials of the cluster, greatly distorts its geometric structure, and reduces the cluster stability in solution. These findings are expected to be useful for developing design guidelines for functionalizing $[\text{Au}_{25}(\text{SR})_{18}]^-$ through doping with foreign atoms.

References

- 1) M. Noda, T. Yasuike, K. Nobusada and M. Hayashi, *Chem. Phys. Lett.* **550**, 52–57 (2012).
- 2) Y. Negishi, K. Igarashi, K. Munakata, W. Ohgake and K. Nobusada, *Chem. Commun.* **48**, 660–662 (2012).
- 3) Y. Negishi, K. Munakata, W. Ohgake and K. Nobusada, *J. Phys. Chem. Lett.* **3**, 2209–2214 (2012).

Advanced Electronic Structure Theory in Quantum Chemistry

Department of Theoretical and Computational Molecular Science
Division of Theoretical Molecular Science I



YANAI, Takeshi
KURASHIGE, Yuki
CHALUPSKY, Jakub
TRAN, Lan
SAITOW, Masaaki
YAMADA, Mariko

Associate Professor
Assistant Professor
IMS Fellow
Graduate Student
Graduate Student*
Secretary

Aiming at predictive computational modelings of molecular electronic structures with *ab initio* quantum chemistry calculations, our scientific exploration is to establish a cutting-edge theoretical methodology that allows one to compute accurately and efficiently the complex electronic structures, in which strongly-interacting electrons play a crucial role to characterize the nature of molecules. The complicated electronic structures can be handled accurately with the multi-reference theory, which deals with multiple important electronic configurations on equal footing. However, with the standard multireference methods such as the complete active space self-consistent field (CASSCF), the tractable size of the reference space is limited to small active space because the complexity of the calculations grows exponentially with the reference size. The existing multireference methods are nevertheless usefully applied to chemical theory problems such as exploring chemical reactions of bonding, dissociation and isomerization along the reaction coordinates, electronically excited states, unstable electronic structures of radical systems, and multiple covalent bindings in molecular metal complexes, *etc.* Our resultant works to be reported here are (1) to develop a type of the multireference correlation model named Canonical Transformation (CT) theory, which can efficiently describe short-range dynamic correlation on top of the multi-configurational starting wave function, (2) to construct the extensive complete active space self-consistent field (CASSCF) method combined with *ab initio* density matrix renormalization group (DMRG) method for making unprecedentedly larger active spaces available for the CASSCF calculations, and (3) to develop an efficient second-order perturbation theory that can use large active space with the DMRG-SCF reference wavefunction.

1. Canonical Transcorrelated Theory with Projected Slater-Type Geminals¹⁾

An effective Hamiltonian perturbed with explicit inter-

Canonical transcorrelated theory

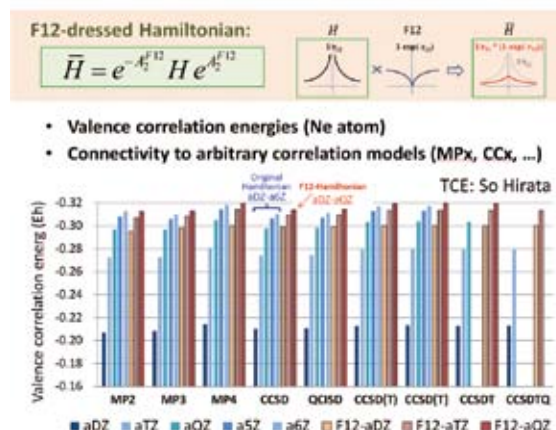


Figure 1. Canonical Transcorrelation method with F12 correlation factor.

electronic correlation is derived from similarity transformation of Hamiltonian using a unitary operator with Slater-type geminals. The Slater-type geminal is projected onto the excitation (and de-excitation) component as in the F12 theory. Simplification is made by truncating higher-body operators, resulting in a correlated Hamiltonian which is Hermitian and has exactly the same complexity as the original Hamiltonian in the second quantized form. It can thus be easily combined with arbitrary correlation models proposed to date. The present approach constructs a singularity-free Hamiltonian *a priori*, similarly to the so-called transcorrelated theory, while the use of the canonical transformation²⁾ assures that the effective Hamiltonian is two-body and Hermite. Our theory is naturally extensible to multireference calculations on the basis of the generalized normal ordering. The construction of the effective Hamiltonian is non-iterative. The numerical assessments demonstrate that the present scheme improves the basis set convergence of the post-mean-field calculations at a similar rate to the explicitly correlated methods proposed by others

that couple geminals and conventional excitations.

In this study, we propose a canonical transcorrelated Hamiltonian with the F12 operator:

$$\hat{H}^{F12} \equiv \hat{H} + \{\hat{H}, \hat{A}^{F12}\}_{1,2} + \frac{1}{2}[\{\hat{F}, \hat{A}^{F12}\}_{1,2}, \hat{A}^{F12}\}_{1,2}$$

which is derived in two ways of formal approximations: (i) terminating the expansion at the second order and (ii) replacing the uncorrelated Hamiltonian \hat{H} at the second order term (*i.e.*, the double commutator) by the Fock operator F . Note that F is the effective one-particle approximation to \hat{H} . This truncation of the infinite expansion is correct through the second order in perturbation.

We use an anti-Hermitian generator with projected geminal functions to make the transcorrelated H Hermite:

$$\begin{aligned} \hat{A}^{F12} &= \frac{1}{2} G_{ij}^{\alpha\beta} (\hat{E}_{ij}^{\alpha\beta} - \hat{E}_{ij}^{\beta\alpha}), \\ G_{ij}^{\alpha\beta} &= \frac{3}{8} \langle \alpha\beta | \hat{Q}_{12} F_{12} | ij \rangle + \frac{1}{8} \langle \alpha\beta | \hat{Q}_{12} F_{12} | j i \rangle, \\ F_{12} &= -\gamma^{-1} \exp(-\gamma r_{12}), \end{aligned}$$

in which we have fixed the amplitudes by those determined by the first-order cusp condition. The explicit electron correlation with the *projected* Slater-type geminals is built into a Hamiltonian through the canonical transformation. The present approach provides a formulation to effectively remove high-energy orbital components by using the F12 factor as a regulator for renormalizing them into the smaller-size orbital space. The features of the canonical transcorrelated theory are:

- (1) The resulting effective Hamiltonian is already perturbed with a considerable amount of the dynamic correlation associated with the interelectronic Coulomb singularity;
- (2) It remains Hermitian and has exactly the same size, dimension, and quartic complexity as the bare Hamiltonian;

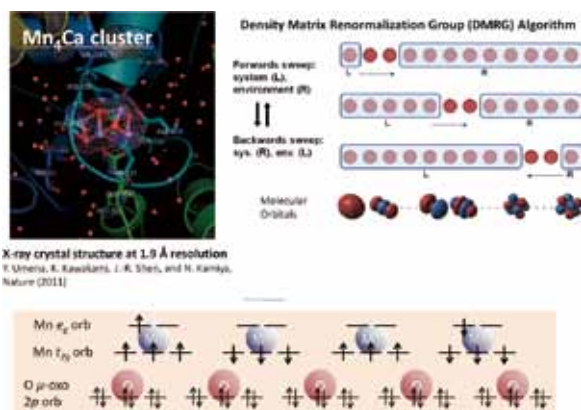


Figure 2. Determination of oxidation state of Mn_4CaO_5 cluster in photosystem II from a multireference wavefunction theory based on Density Matrix Renormalization Group method.

- (3) There is no adjustable parameter in the geminal excitations with Ten-no's fixed amplitude ansatz, since the F12 amplitudes for the present transformation are predetermined and calculated in a non-iterative manner;
- (4) The theory is extensible to multireference models on the basis of the generalized normal ordering of Mukherjee and Kutzelnigg;
- (5) In contrast to the standard F12 theories which couple the F12 and conventional excitations in the amplitude equations or Valeev's *a posteriori* F12 corrections, we have introduced an *a priori* F12 transformed Hamiltonian that can be readily used in conjunction with arbitrary correlation models to describe the remaining orbital correlation. We have demonstrated its applications to various solvers in quantum chemical methods, such as CCSD(T), QCISD, MP4, CCSDT, CCSDTQ, and so forth. The benchmarks on small molecules have revealed that the numerical performance of our explicit correlation scheme is comparable to that of other F12 theories. In our method, the F12 correction and the orbital correlation are treated separately at different steps, and thus it is indicated that they are more or less additively separable. (**Figure 1**)

2. Oxidation State of Mn_4Ca Cluster in Photosystem II: A Quantum-Chemical Density-Matrix Renormalization Group Study³

The X-ray diffraction (XRD) structure of photosystem II at a resolution of 1.9 Å was recently reported, entailing atomic-details of the Mn_4Ca cluster. Meanwhile, there is an earlier study suggesting that the high-valent Mn^{III-IV} ions of the cluster are potentially damaged by X-rays and reduced towards the lower-valent Mn^{II} , involving structural deformation. Thus, the record-resolution XRD measurement used a low-level X-ray dose to avoid such damage. We report a theoretical analysis identifying the oxidation states of the Mn ions as fingerprints to be compared with the widely-accepted oxidation state. Super high-dimensional multireference wavefunctions were calculated to account for nonperturbative interactions arising from four Mn 3d and five μ -oxo 2p shells. (**Figure 2**)

References

- 1) T. Yanai and T. Shiozaki, *J. Chem. Phys.* **136**, 084107 (9 pages) (2012).
- 2) T. Yanai, Y. Kurashige, E. Neuscammann and G. K.-L. Chan, *Phys. Chem. Chem. Phys.* **14**, 7809–7820 (2012).
- 3) Y. Kurashige, G. K.-L. Chan and T. Yanai, submitted.

* carrying out graduate research on Cooperative Education Program of IMS with Rikkyo University

Developing the Statistical Mechanics Theory of Liquids in Chemistry and Biophysics

Department of Theoretical and Computational Molecular Science
Division of Theoretical Molecular Science II



HIRATA, Fumio Professor (–March, 2012)*
YOSHIDA, Norio Assistant Professor†
MARUYAMA, Yutaka Post-Doctoral Fellow
PHONGPHANPHANEE, Saree Post-Doctoral Fellow
SINDHIKARA, Daniel J. Post-Doctoral Fellow
KIYOTA, Yasuomi Post-Doctoral Fellow
SUETAKE, Yasumi Secretary
KONDO, Naoko Secretary
YAMADA, Mariko Secretary

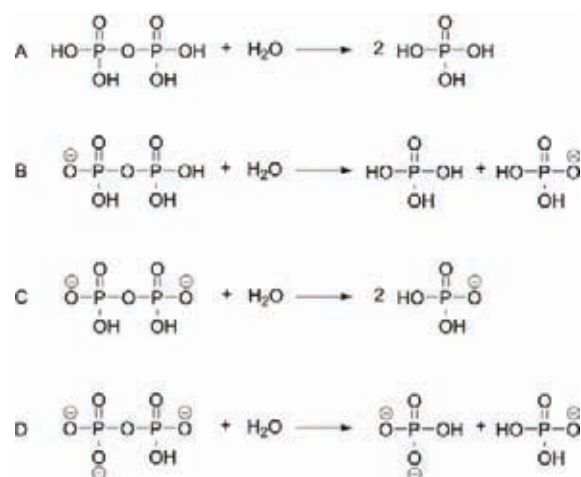
“Molecular recognition” is an essential elementary process for protein to function. The process is a thermodynamic process which is characterized with the free energy difference between two states of a host-guest system, namely, associated and dissociated states. It is readily understood that the structural fluctuation of protein gives a big effect on the free energy barrier. In that respect, the “molecular recognition” is a thermodynamic process which is conjugated with the structural fluctuation of protein.

We have been developing a new theory concerning the molecular recognition, based on the 3D-RISM/RISM theory which is a statistical mechanics of liquids. The theory has successfully “probed” small ligands such as water molecules and ions bound in a small cavity of protein.^{1–3)}

1. Elucidating the Molecular Origin of Hydrolysis Energy of Pyrophosphate in Water⁴⁾

The molecular origin of the energy produced by the ATP hydrolysis has been one of the long-standing fundamental issues. A classical view is that the negative hydrolysis free energy of ATP originates from intra-molecular effects connected with the backbone P–O bond, so called “high-energy bond.” On the other hand, it has also been recognized that solvation effects are essential in determining the hydrolysis free energy. Here, using the 3D-RISM-SCF (three-dimensional reference interaction site model self-consistent field) theory that integrates the ab initio quantum chemistry method and the statistical mechanical theory of liquids, we investigate the molecular origin of hydrolysis free energy of pyrophosphate, an ATP analog, in water. We demonstrate that our theory quantitatively reproduces the experimental results without the use of empirical parameters. We clarify the crucial role of water in converting the hydrolysis free energy in the gas phase determined solely by intra-molecular effects, which ranges from endothermic, thermoneutral to highly exothermic depending on the charged state of pyrophosphate, into moderately

exothermic in the aqueous phase irrespective of the charged state as observed in experimental data. We elucidate that this is brought about by different natures of solute–water interactions depending on the charged state of solute species: the hydration free energy of low-charged state is mainly subjected to short-range hydrogen-bonds, while that of high-charged state is dominated by long-range electrostatic interactions. We thus provide unambiguous evidence on the critical role of water in determining the ATP hydrolysis free energy.



Scheme 1. Schematic description of the hydrolysis reaction of pyrophosphate for the four possible charged states.

Table 1. The reaction free energies in the gas phase and in the aqueous phase at 298.15 K and 1.0 atm computed by DFT at the B3LYP/6-31+(d) level and the 3D-RISM-SCF theory. Units are in kcal/mol.

Reaction	gas phase (DFT)	aqueous phase (3D-RISM/RISM)	Exp.
A	–1.7	–8.9	–9.5
B	21.3	–6.2	–7.5
C	–56.6	–8.1	–7.7
D	–119.0	–7.7	–7.1

2. Placevent: An Algorithm for Predicting of Explicit Solvent Atom Distribution—Application to HIV-1 Protease and F-ATP Synthase⁵⁾

Location of water and ions in native structure of protein is of essential importance for its stability and for its functions. However, determination of the position of those species in protein is not an easy task for any experimental methods currently available, X-ray, NMR, neutron diffraction, and the molecular simulation.

We have created a simple algorithm for automatically predicting the explicit solvent atom distribution of biomolecules. The explicit distribution is coerced from the 3D continuous distribution resulting from a 3D-RISM calculation. This procedure predicts optimal location of solvent molecules and ions given a rigid biomolecular structure and the solvent composition. We show examples of predicting water molecules near the KNI-272 bound form of HIV-1 protease and predicting both sodium ions and water molecules near the rotor ring of F-ATP synthase. Our results give excellent agreement with experimental structure with an average prediction error of 0.45–0.65 Å. Further, unlike experimental methods, this method does not suffer from the partial occupancy limit. Our method can be performed directly on 3D-RISM output within minutes. It is extremely useful for examining multiple specific solvent–solute interactions, as a convenient method for generating initial solvent structures for MD calculations, and may assist in refinement of experimental structures.

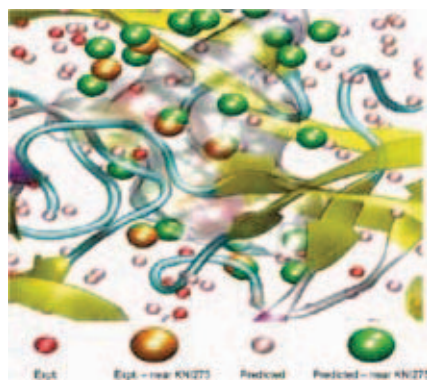


Figure 1. Water molecules near KNI-275. KNI-275 is shown as a translucent surface, HIV-1 protease as a cartoon. Crystal water molecules near KNI-275 are shown in orange, elsewhere in red. Water molecules placed by this method near KNI-275 are shown in green, elsewhere in pink.

3. Modified Andersen Method for Accelerating 3D-RISM Calculations Using Graphics Processing Unit⁶⁾

Increasing attention has been paid to the 3D-RISM theory due mainly to its capability of treating “solvation” of bio-

molecules such as protein and DNA without using any adjustable parameters, which is the case in the continuum model. The method was highlighted in several symposiums in the latest ACS meeting held in Philadelphia. Superiority of 3D-RISM to the continuum models, the Poisson-Boltzmann and generalized Born equations, was addressed unambiguously by several talks in the symposiums as far as physical soundness, amount of information produced, applicability to drug design, and so on, are concerned. However, there still remains one point which makes people stick to the continuum models. That is the computation cost. The cost to perform the 3D-RISM calculation is far higher than that of the continuum models. We have proposed a fast algorithm to solve the 3D-RISM equation on a graphics processing unit (GPU). It was the large memory space required for convergence of iteration that banned 3D-RISM from GPU. In order to overcome the difficulty, we replaced the conventional MDIIS algorithm by Anderson’s method with some modification. Using this method on a Tesla C2070 GPU, we reduced the total computational time by a factor of eight, 1.4 times by the modified Andersen method and 5.7 times by GPU, compared to calculations on an Intel Xeon machine (8 cores, 3.33 GHz) with the conventional method.

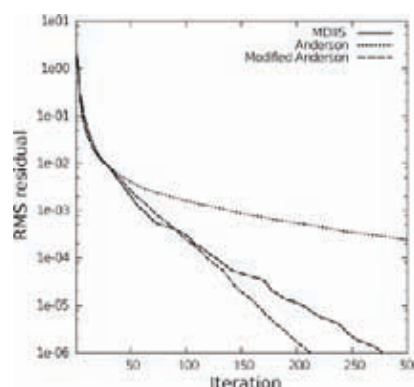


Figure 2. Root mean square residual against the number of iteration steps for the calculation of 3D site distribution profiles of water around a DNA molecule by 3D-RISM. Solid, dotted, and dashed lines are for MDIIS, Anderson, and Modified Anderson algorithms, respectively.

References

- 1) F. Hirata, *Molecular Theory of Solvation*, Kluwer; Dordrecht, Netherlands (2003).
- 2) A. Kovalenko and F. Hirata, *J. Chem. Phys.* **110**, 10095–10112 (1999).
- 3) T. Imai, R. Hiraoka, A. Kovalenko and F. Hirata, *J. Am. Chem. Soc. (Communication)* **127**, 15334–15335 (2005).
- 4) J. Hong, N. Yoshida, S.-H. Chong, C. Lee, S. Ham and F. Hirata, *J. Chem. Theory Comput.* **8**, 2239 (2012).
- 5) D. Sindhiara, N. Yoshida and F. Hirata, *J. Comput. Chem.* **33**, 1536 (2012).
- 6) Y. Maruyama and F. Hirata, *J. Chem. Theory Comput.* **8**, 2239–2246 (2012).

* Present Address; College of Life Sciences, Ritsumeikan University

† Present Address; Graduate School of Sciences, Kyushu University

Theory of Photoinduced Phase Transitions

Department of Theoretical and Computational Molecular Science
Division of Theoretical Molecular Science II



YONEMITSU, Kenji
TANAKA, Yasuhiro
NISHIOKA, Keita
MIYAZAKI, Mitake
KONDO, Naoko

Associate Professor (–March, 2012)*
Assistant Professor
IMS Fellow[†]
Visiting Scientist[‡]
Secretary

Photoirradiation of materials usually creates electrons and holes, which are often accompanied by local structural deformation. With the help of cooperativity, the electronic and/or structural deformation can proliferate to change the physical property such as conductivity, permittivity, and magnetic susceptibility. The resultant nonequilibrium phase may not be reached by changing temperature or pressure because the energy of a photon is much higher than thermal energies. Our theoretical researches are focused on the mechanisms and dynamics of photoinduced phase transitions, how they are controlled, and how the photoinduced electron–lattice states are different from those which are realized in thermal equilibrium.¹⁾

1. Normal Mode Analysis for Intra- and Inter-Molecular Electron–Phonon Coupled Systems

The ground-state properties of a molecular compound $\text{Et}_2\text{Me}_2\text{Sb}[\text{Pd}(\text{dmit})_2]$ are theoretically studied, which shows a dimer-Mott character in $\text{Pd}(\text{dmit})_2$ layers at high temperature and charge order mainly stabilized by electron–phonon interactions at low temperature. An effective extended Peierls-Hubbard model is constructed with intra- and inter-molecular electronic and phonon degrees of freedom. Using a mean-field approximation, the energies and optimized structures are calculated for isolated neutral, monovalent, divalent $\text{Pd}(\text{dmit})_2$ dimers and their two-dimensional crystallized states. The optical conductivities of the latter are calculated by a single configuration interaction method. Through these numerical calculations, model parameters have been evaluated by comparing the theoretical and experimental ground-state properties.

Then, the normal mode analysis is performed for the intradimer C=C stretching vibrations and intradimer inter-monomer stretching vibrations. Molecular vibrations with different symmetries are coupled to different combinations of electrons and holes within a molecule, so that their frequencies depend on the molecular charge in different manners. This

information is useful to analyze photoinduced transient states, where the relation between their frequencies and the molecular charge is modified from the equilibrium counterpart.

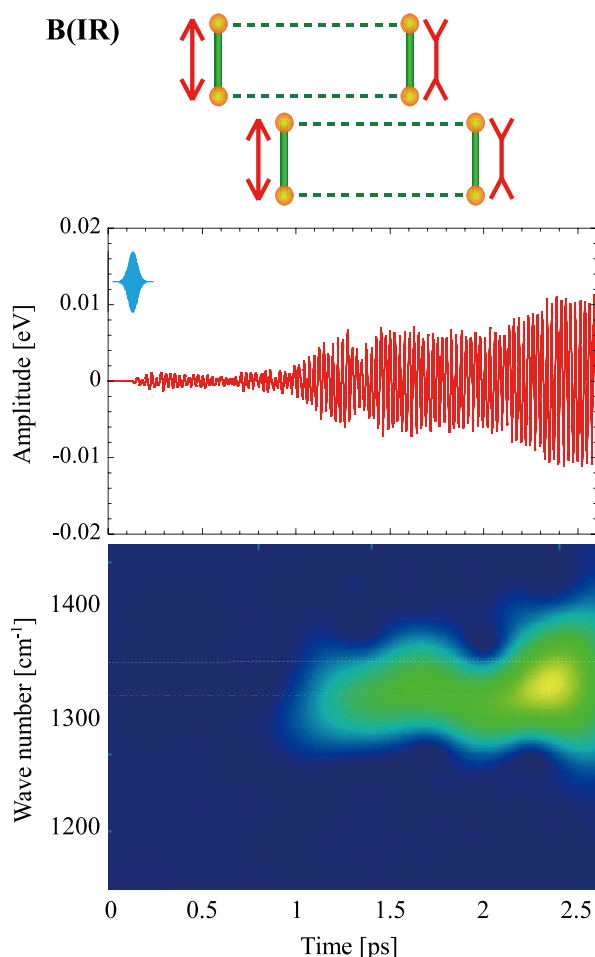


Figure 1. C=C stretching phonon mode B (infrared active) schematically represented in the upper panel. Its time evolution (middle panel) and time-frequency spectrogram (lower panel) on the initially neutral dimer are shown when the charge-separated state is photoexcited.

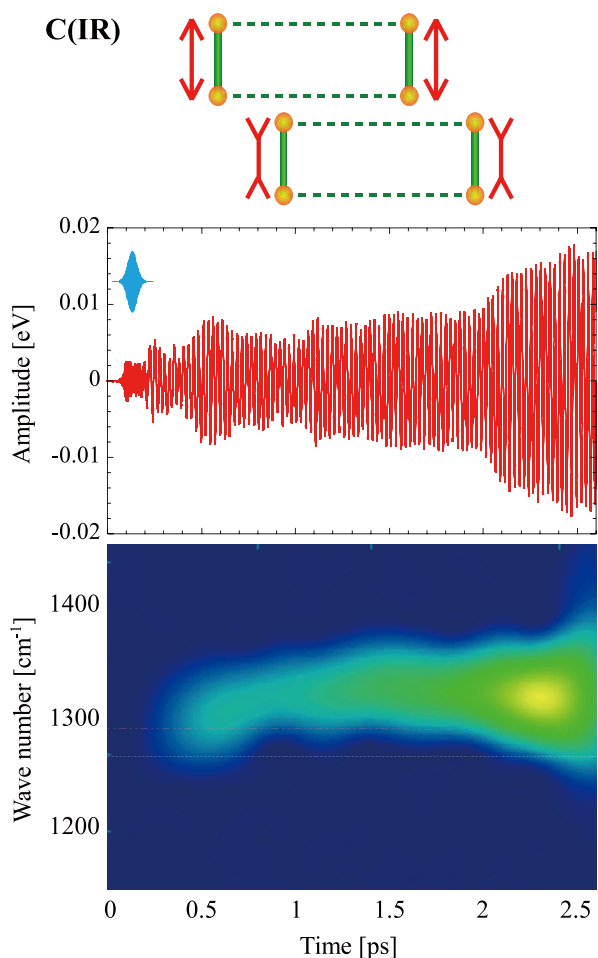


Figure 2. C=C stretching phonon mode C (infrared active) schematically represented in the upper panel. Its time evolution (middle panel) and time-frequency spectrogram (lower panel) on the initially neutral dimer are shown when the charge-separated state is photoexcited.

2. Photoinduced Dynamics in Intra- and Inter-Molecular Electron-Phonon Coupled Systems²⁾

For the photoinduced dynamics in $\text{Et}_2\text{Me}_2\text{Sb}[\text{Pd}(\text{dmit})_2]_2$, the time-dependent Schrödinger equation is numerically solved for the Hartree-Fock wave function on the cluster of sixteen dimers (eight sites in each dimer, 128 sites in total). The

classical equation of motion is solved for phonons. Photoexcitation is introduced through the Peierls phase in the transfer integrals.

We focus on intradimer C=C stretching vibrations that are infrared active and experimentally observed so far, which are schematically shown in the upper panels of Figures 1 and 2. The middle panels show the time evolution of their amplitudes on the initially neutral dimer when the charge-separated state is photoexcited. The lower panels show their time-frequency spectrograms.

The initially neutral and divalent dimers become monovalent at about 0.5 ps after photoexcitation. After 0.5 or 1 ps, their oscillations are noticeable and sinusoidal. The frequency of the B mode is actually close to that in a monovalent dimer in the equilibrium state. The B mode is coupled with the antibonding-LUMO (electron)–antibonding-HOMO (hole) excitation within the dimer. Their correlation is recovered and becomes close to that in equilibrium after 1 ps.

However, the frequency of the C mode after 1 ps is not close to that in a neutral dimer or that in a monovalent dimer, but it is rather close to the bare frequency (*i.e.*, the frequency if the couplings with electron–hole excitations are turned off) of 1331 cm^{-1} . The C mode is coupled with the antibonding-HOMO (electron)–bonding-HOMO (hole) excitation and the antibonding-LUMO (electron)–bonding-LUMO (hole) excitation within the dimer, so that it is largely softened in equilibrium. Their correlations are largely modified and far from that in equilibrium after 1 ps. This phonon mode appears to oscillate almost independently of electron–hole excitations.

Thus, a usual picture based on the adiabatic potential fails even if phonons are treated classically. The correlation between a phonon and its relevant electron–hole excitation(s) depends on the mode or on the symmetries of the vibrational pattern and the wave functions of electron(s) and hole(s). The analysis of these correlations at an early stage of photoinduced charge-order melting is essential for future manipulation of non-equilibrium phases.

References

- 1) K. Yonemitsu, *Crystals* **2**, 56–77 (2012).
- 2) K. Nishioka and K. Yonemitsu, *Phys. Status Solidi C* **9**, 1213–1215 (2012).

* Present Position; Professor, Department of Physics, Faculty of Science and Engineering, Chuo University, 1-13-27 Kasuga, Bunkyo-ku, Tokyo 112-8551

† Present Address; Department of Physics, Faculty of Science and Engineering, Chuo University, 1-13-27 Kasuga, Bunkyo-ku, Tokyo 112-8551

‡ from Hakodate National College of Technology

Theoretical Studies on Condensed Phase Dynamics

Department of Theoretical and Computational Molecular Science
Division of Computational Molecular Science



SAITO, Shinji	Professor
KIM, Kang	Assistant Professor
HIGASHI, Masahiro	JSPS Post-Doctoral Fellow
YAGASAKI, Takuma	Post-Doctoral Fellow
IMOTO, Sho	Graduate Student
KAWAGUCHI, Ritsuko	Secretary

Liquids and biological systems show complicated dynamics because of their structural flexibility and dynamical hierarchy. Understanding these complicated dynamics is indispensable to elucidate chemical reactions and relaxation in solutions and functions of proteins. In this year, we investigated ultrafast proton transfer in solution¹⁾ and dynamics of liquid and supercooled states.²⁻⁵⁾ In particular, we examined complicated dynamics in terms of nonlinear response functions and multi-time correlation functions.

1. Direct Simulation of Excited-State Intramolecular Proton Transfer and Vibrational Coherence of 10-Hydroxybenzo[*h*]quinoline in Solution¹⁾

We investigate an ultrafast excited-state intramolecular proton transfer (ESIPT) reaction and the subsequent coherent vibrational motion of 10-hydroxybenzo-*[h]*quinoline in cyclohexane by the electronically embedded multiconfiguration Shepard interpolation method, which enables us to generate the potential energy surface of the reaction effectively and thus carry out a direct excited-state dynamics simulation with low computational costs. The calculated time scale of the ESIPT and the frequencies and lifetimes of coherent motions are in good agreement with the experimental results. The present study reveals that the coherent motions are caused by not only the proton transfer itself but also the backbone displacement induced by the ESIPT. We also discuss the effects of the solvent on the dynamics of the coherent vibrational modes.

2. Insights in Quantum Dynamical Effects in the Infrared Spectroscopy of Liquid Water from a Semiclassical Study with an *Ab Initio*-Based Flexible and Polarizable Force Field²⁾

The dynamical properties of liquid water play an important role in many processes in Nature. In this paper we focus on the infrared (IR) absorption spectrum of liquid water based on the linearized semiclassical initial value representation (LSC-IVR) with the local Gaussian approximation (LGA) [Liu and Miller, *J. Chem. Phys.* **131**, 074113 (2009)] and an *ab initio* based, flexible, polarizable Thole-type model (TTM3-F) [Fanourgakis and Xantheas, *J. Chem. Phys.* **128**, 074506 (2008)]. Although the LSC-IVR (LGA) gives the exact result for the isolated 3-dimensional shifted harmonic stretching model, it yields a blue-shifted peak position for the more realistic anharmonic stretching potential. By using the short time information of the LSCIVR correlation function, however, it is shown how one can obtain more accurate results for the position of the stretching peak. Due to the physical decay in the condensed phase system, the LSC-IVR (LGA) is a good and practical approximate quantum approach for the IR spectrum of liquid water. The present results offer valuable insight into future attempts to improve the accuracy of the TTM3-F potential or other *ab initio*-based models in reproducing the IR spectrum of liquid water.

3. Energy Relaxation of Intermolecular Motions in Supercooled Water and Ice: A Molecular Dynamics Study³⁾

We investigate the energy relaxation of intermolecular motions in liquid water at temperatures ranging from 220 K to 300 K and in ice at 220 K using molecular dynamics simulations. We employ the recently developed frequency resolved transient kinetic energy analysis, which provides detailed information on energy relaxation in condensed phases like two-color pump-probe spectroscopy. It is shown that the energy cascading in liquid water is characterized by four processes. The temperature dependences of the earlier three processes, the rotational–rotational, rotational–translational, and translational–translational energy transfers, are explained in terms of the density of states of the intermolecular motions. The last process is the slow energy transfer arising from the transitions between potential energy basins caused by the excitation of the low frequency translational motion. This process is absent in ice because the hydrogen bond network rearrangement, which accompanies the interbasin transitions in liquid water, cannot take place in the solid phase. We find that the last process in supercooled water is well approximated by a stretched exponential function. The stretching parameter, β , decreases from 1 to 0.72 with decreasing temperature. This result indicates that the dynamics of liquid water becomes heterogeneous at lower temperatures.

4. Fluctuations and Dynamics of Liquid Water Revealed by Nonlinear Spectroscopy⁴⁾

Many efforts have been devoted to elucidate the intra- and intermolecular dynamics in liquid water because of its important roles in many fields of science and engineering. Multi-dimensional nonlinear spectroscopy is a powerful tool to investigate the dynamics. Since nonlinear response functions are described by more than one time variable, it is possible to analyze static and dynamic mode couplings. Here, we review the intra- and intermolecular dynamics of liquid water revealed by recent nonlinear spectroscopic experiments and computer simulations. In particular, we discuss the anharmonic coupling, population relaxation, anisotropy decay, and spectral diffusion of intra- and intermolecular motions of water and their temperature dependence, which play important role in ultrafast dynamics and relaxations in water.

5. Anomalous Temperature Dependence of Isobaric Heat Capacity of Water below 0 °C⁵⁾

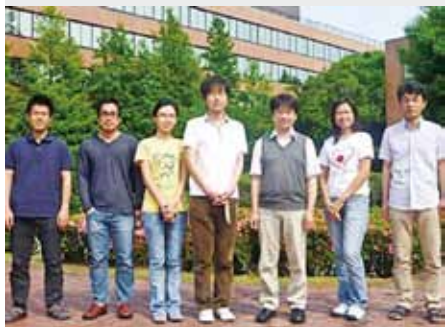
When pure liquid water is cooled below its freezing/melting temperature, it exhibits a number of striking anomalies. Most remarkable among these anomalies is the temperature dependence of the isobaric heat capacity, C_P , that exhibits first a rise, and then a fall, on lowering temperature substantially below 0 °C.^{1–4)} In contrast, the isochoric heat capacity, C_V , remains weakly temperature dependent and displays no such anomaly. The reason for this surprisingly large difference is not well understood. To understand this and other anomalies of low temperature water, we examine both *wave number and frequency dependent temperature fluctuation* by long molecular dynamics simulations. Significant differences between constant pressure and constant volume conditions appear below 240 K in the spatio-temporal correlation of temperature fluctuation. Shell-wise decomposition of relative contribution to the temperature fluctuation reveals an increase in contribution from the distant regions, extending even up to the *fifth hydration shell, at low temperatures*, more significant under isobaric than under isochoric conditions. While the temperature fluctuation time correlation function (TFCF) exhibits the expected slow-down with lowering temperature, it shows a rather surprisingly sharp crossover from a markedly fragile to a weakly fragile liquid around 220 K. We establish that this crossover of TFCF (and the related anomalies) arises from a percolation transition in the population of clusters made of liquid-like molecules, defined by coordination number (and consistent with local volumes obtained from Voronoi polyhedra). The disappearance of large liquid-like clusters below 220 K display characteristic features consistent with theory⁵⁾ of percolation. As temperature is further lowered, TFCF exhibits a power law decay and the relaxation time, when fitted to Vogel-Fulcher-Tammann law, reveal a dynamic transition around 160–170 K. Our computed two-dimensional IR and Raman spectra both also signal a dynamical transition around 170 K and additionally carry signatures of the percolation transition at 220 K that could be measured experimentally.

References

- 1) M. Higashi and S. Saito, *J. Phys. Chem. Lett.* **2**, 2366–2371 (2011).
- 2) J. Liu, W. H. Miller, G. S. Fanourgakis, S. S. Xantheas, S. Imoto and S. Saito, *J. Chem. Phys.* **135**, 244503 (14 pages) (2011).
- 3) T. Yagasaki and S. Saito, *J. Chem. Phys.* **135**, 244511 (2011).
- 4) T. Yagasaki and S. Saito, *Annu. Rev. Phys. Chem.*, submitted.
- 5) S. Saito, I. Ohmine, and B. Bagchi, submitted.

Theoretical Study on Molecular Excited States and Chemical Reactions

Department of Theoretical and Computational Molecular Science
Division of Computational Molecular Science



EHARA, Masahiro	Professor
FUKUDA, Ryoichi	Assistant Professor
TASHIRO, Motomichi	IMS Research Assistant Professor
BOBUATONG, Karan	Post-Doctoral Fellow*
CHITHONG, Rungtiwa	Visiting Scientist
MAITARAD, Phornphimon	Visiting Scientist
MEEPASERT, Jittima	Visiting Scientist
HORIKAWA, Takenori	Graduate Student
PROMKATKAEW, Malinee	Graduate Student†
KAWAGUCHI, Ritsuko	Secretary

Molecules in the excited states show characteristic photo-physical properties and reactivity. We investigate the molecular excited states and chemical reactions which are relevant in chemistry, physics, and chemical biology with developing the highly accurate electronic structure theory. We are also interested in the excited-state dynamics and energy relaxation so that we also develop the methodology of large-scale quantum dynamics. In this report, we present our recent studies on the development of the CAP/SAC-CI method,¹⁾ electronic spectra of annulated dinuclear free-base phthalocyanine,²⁾ and aerobic oxidation of methanol to formic acid on Au₂₀⁻ cluster.³⁾

1. Development of CAP/SAC-CI Method for Calculating Resonance States of Metastable Anions¹⁾

A “resonance” is an electronically metastable state, that is, a state of an ($N+1$)-electron system that lies energetically above the ground state of the associated N -electron system and can consequently decay by electron autodetachment. Resonances are intermediates in electron-induced processes and electron-catalyzed reactions. Resonances are part of the continuum and are represented by non-square-integrable (non- L^2) wavefunctions. Computational methods for resonances are thus necessarily combinations of a method to address the continuum nature of the state and a method to address its many-body nature. It is this combination that renders computing the resonance parameters, E_r and τ , of a many-electron system a challenging task.

In this work, we have developed the complex absorbing potential (CAP)/SAC-CI method to investigate resonance states of metastable anions. The method has been implemented in the projected scheme and applied to the π^* resonance state of formaldehyde. The dependence on both valence and diffuse basis sets up to g -function, the number of SAC-CI states in the projection, and the effect of perturbation selection are examined. The potential energy curve and decay width are calculated in the C–O stretching coordinate (Figure 1), and the Franck-Condon factors for transitions from neutral to resonance state

are evaluated to interpret the electron transmission (ET) spectrum. (Figure 2)

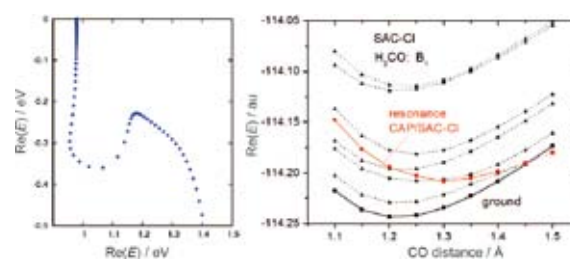


Figure 1. η -trajectory of the 2B_1 resonance state of H₂CO (left) and potential energy curves of the ground, electron-attached 2B_1 states, and the π^* resonance state by the projected CAP/SAC-CI (right).

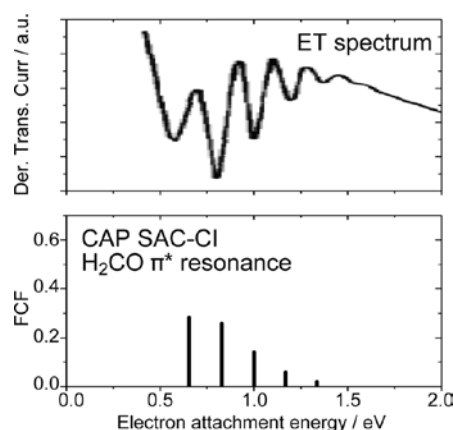


Figure 2. Vibrational structure in π^* resonance of H₂CO by the projected CAP/SAC-CI method compared with the electron transmission spectrum.

2. Electronic Spectra of Annulated Dinuclear Free-Base Phthalocyanines²⁾

There are many applications for organic dyes with strong photoabsorption in the near-IR region, including photo-energy conversion, molecular sensors and devices, and biological

applications. A reliable theory that can treat large conjugated system is urgently required for molecular designs and analysis of the electronic structure of near-IR absorbing materials. The direct SAC-CI method is accurate and efficient for studying large conjugated molecules.

The electronic excited states and electronic absorption spectra of annulated dinuclear free-base phthalocyanine ($C_{58}H_{30}N_{16}$) are studied through quantum chemical calculations using the SAC-CI method. Three tautomers are possible with respect to the position of the pyrrole protons; therefore, the SAC-CI calculations for these tautomers were performed. The lower energy shift of the Q-bands because of dimerization is explained by the decrease in the HOMO–LUMO gaps resulting from the bonding and antibonding interactions between the monomer units. The relative energies of these tautomers are examined using DFT calculations for several peripheral substituents. The relative energies of these tautomers significantly depend on the substituents, and therefore, the abundance ratios of the three tautomers were affected by the substituents. The absorption spectra were simulated from the SAC-CI results weighted by the Boltzmann factors obtained from the DFT calculations. The SAC-CI spectra reproduce the experimental findings well. The thermal-averaged SAC-CI spectra could explain the observed substituent effect on the structure of the Q-bands in terms of the relative stabilities and the abundance ratios of the tautomers.

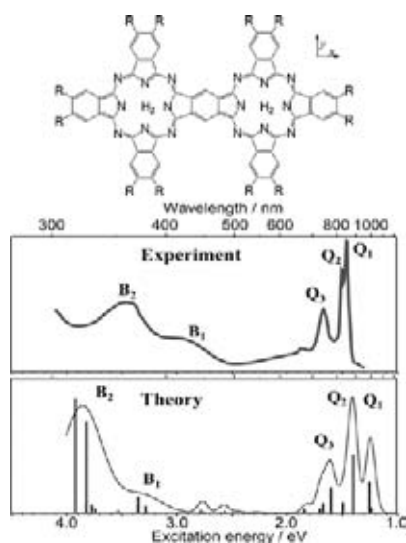


Figure 3. Molecular structure of annulated dinuclear free-base phthalocyanine and its electronic absorption spectra.

3. Aerobic Oxidation of Methanol to Formic Acid on Au_{20}^- Cluster³⁾

During the past two decades, the chemical transformation of hydrocarbons catalyzed by nanometer-sized gold clusters has been of significant interest in industrial and academic research because of its remarkable potential for green chem-

istry and economic significance. Useful and practical reactions with gold catalysts have been extensively developed since the pioneering work of Haruta and co-workers. Among these reactions, aerobic oxidation (oxidation with molecular oxygen) on gold clusters has received special attention because it enables us to perform such reactions at ambient conditions and low temperatures, providing high selectivity to the desired products.

In this work, we investigated the aerobic oxidation of methanol to formic acid catalyzed by Au_{20}^- using density functional theory with the M06 functional. Possible reaction pathways are examined taking account of full structure relaxation of the Au_{20}^- cluster. The proposed reaction mechanism consists of three elementary steps (Figure 4): (1) formation of formaldehyde from methoxy species activated by a superoxo-like anion on the gold cluster; (2) nucleophilic addition by the hydroxyl group of a hydroperoxyl-like complex to formaldehyde resulting in a hemiacetal intermediate; and (3) formation of formic acid by hydrogen transfer from the hemiacetal intermediate to atomic oxygen attached to the gold cluster. A comparison of the computed energetics of various elementary steps indicates that C–H bond dissociation of the methoxy species leading to formation of formaldehyde is the rate-determining step. A possible reaction pathway involving single-step hydrogen abstraction, a concerted mechanism, is also discussed. The stabilities of reactants, intermediates and transition state structures are governed by the coordination number of the gold atoms, charge distribution, cooperative effect and structural distortion, which are the key parameters for understanding the relationship between the structure of the gold cluster and catalytic activity in the aerobic oxidation of alcohol.

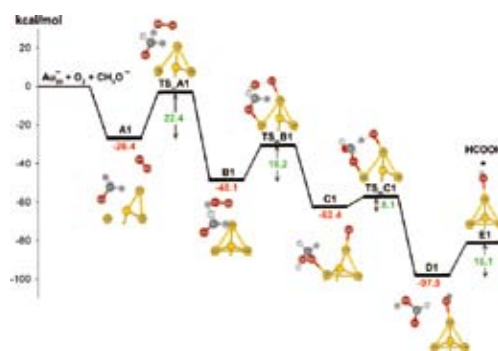


Figure 4. Energy diagram of reaction pathway I in the aerobic oxidation of methanol to formic acid on Au_{20}^- (kcal/mol).

References

- 1) M. Ehara and T. Sommerfeld, *Chem. Phys. Lett.* **537**, 107–112 (2012).
- 2) R. Fukuda and M. Ehara, *J. Chem. Phys.* **136**, 114304 (15 pages) (2012).
- 3) K. Bobuatong, S. Karanjit, R. Fukuda, M. Ehara and H. Sakurai, *Phys. Chem. Chem. Phys.* **14**, 3103–3111 (2012).

* Present Address; Kasetsart University, Bangkok, 10330, Thailand

† carrying out graduate research on Cooperative Education Program of IMS with Kasetsart University

Development of New Algorithms for Molecular Dynamics Simulation and Its Application to Biomolecular Systems

Department of Theoretical and Computational Molecular Science
Division of Computational Molecular Science



OKUMURA, Hisashi	Associate Professor
ITO, G. Satoru	Assistant Professor
MORI, Yoshiharu	IMS Research Assistant Professor
NOMURA, Hitomi	Graduate Student*
KAWAGUCHI, Ritsuko	Secretary

In the conventional canonical-ensemble simulations, it is difficult to realize efficient samplings in proteins because the simulations tend to get trapped in a few of many local-minimum states. To overcome these difficulties, we have proposed new generalized-ensemble algorithms, such as multibaric-multithermal algorithm, partial multicanonical algorithm, van der Waals replica exchange method, and Coulomb replica exchange method. It is important to realize efficient samplings in the conformational space and to predict the native structures of proteins. We apply these methods to proteins and peptides.

1. Temperature and Pressure Denaturation of Chignolin: Folding and Unfolding Simulation by Multibaric-Multithermal Molecular Dynamics Method

We performed a multibaric-multithermal molecular dynamics (MD) simulation of a 10-residue protein, chignolin and discussed its folding thermodynamics last year. We further investigated the denaturation mechanisms this year.¹⁾

All-atom model for the protein with Amber parm99SB force field were employed in explicit TIP3P water. This MD simulation covered wide ranges of temperature between $T = 260\sim 560$ K and pressure between $P = 0.1\sim 600$ MPa and sampled many conformations without getting trapped in local-minimum free-energy states.

Radial distribution function $g(r)$ between the chignolin heavy atoms and the water oxygen atoms, the first peak position of $g(r)$, r_1 , the number of hydration water molecules, and the number of hydrophobic contacts were calculated. As the temperature increases, r_1 increases and the number of

water molecules around chignolin decreases. It represents that chignolin gains more space to move around and is transferred to a high entropy state, even if it losses potential energy by breaking hydrogen bonds between the protein atoms or between the protein and water. Entropy of the transition state and the unfolded state is higher than the native state. This is the reason why the probabilities of not only the unfolded state such as the extended structure but also the transition state increase as the temperature increases.

On the other hand, the number of hydration water molecules increases with the increasing pressure. There are fewer water molecules near the hydrophobic residues when the protein is folded at the room pressure. As the pressure increases, more water molecules come closer to the hydrophobic residues and the number of hydrophobic contacts decreases. The hydrophobic residues then get separated from one another and the protein is unfolded.

2. Coulomb Replica-Exchange Method: Handling Electrostatic Attractive and Repulsive Forces for Biomolecules

We propose a new type of the Hamiltonian replica-exchange method for molecular dynamics (MD) and Monte Carlo simulations, which we refer to as the Coulomb replica-exchange method. In this method, electrostatic charge parameters in the Coulomb interactions are exchanged among replicas while temperatures are exchanged in the usual replica-exchange method. By varying the atom charges, the Coulomb replica-exchange method overcomes free-energy barriers and realizes more efficient sampling in the conformational space than the

replica-exchange method. Furthermore, this method requires only a smaller number of replicas because only the atom charges of solute molecules are employed as exchanged parameters.

We performed Coulomb replica-exchange MD simulations of an alanine dipeptide in explicit water solvent and compared the results with those of the conventional canonical, replica-exchange, and van der Waals replica-exchange methods. Two force fields of AMBER parm99 and AMBER parm99SB were employed. As a result, the Coulomb replica-exchange method sampled all local-minimum free-energy states more frequently than the other methods for both force fields. Moreover, the Coulomb, van der Waals, and usual replica-exchange methods were applied to a fragment of an amyloid- β peptide ($A\beta$) in explicit water solvent to compare the sampling efficiency of these methods for a larger system. The Coulomb replica-exchange method sampled structures of the $A\beta$ fragment more efficiently than the other methods. We obtained β -helix, α -helix, 3_{10} -helix, β -hairpin, and β -sheet structures as stable structures and revealed pathways of conformational transitions among these structures from a free-energy landscape, as shown in Figure 1.

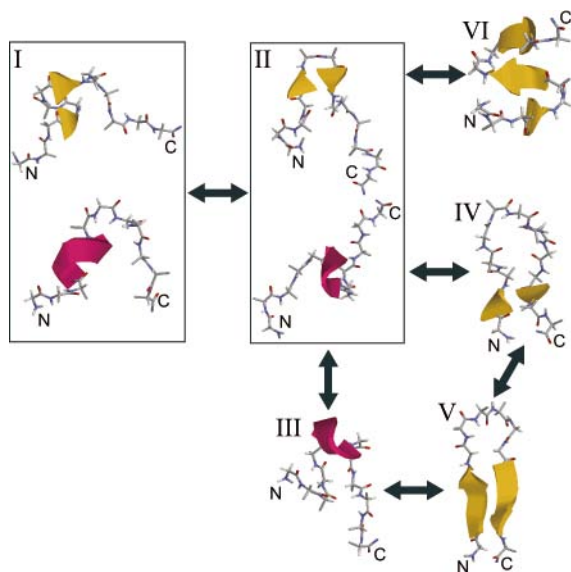


Figure 1. Folding pathways of amyloid- β peptide obtained from Coulomb replica-exchange MD simulations.

3. Replica Exchange Molecular Dynamics Simulation of Chitosan for Drug Delivery System Based on Carbon Nanotube

Chitosan is an important biopolymer in the medical applications because of its excellent biocompatibility. It has been

recently highlighted in the targeted drug delivery system (DDS) by improvement of the carbon nanotube (CNT) solubility. To investigate the effect of chitosan length, the two targeted DDSs with 30 and 60 chitosan monomers were performed by replica-exchange molecular dynamics simulations at temperatures in the range of 300–455 K. Each DDS model contains the epidermal growth factor (EGF), chitosan (CS) of 30 (30CS) and 60 (60CS) monomers, single-wall CNT (SWCNT) and gemcitabine (Gemzar) as the model payload anticancer drug, called EGF/30CS/SWCNT/Gemzar and EGF/60CS/SWCNT/Gemzar, respectively. The SWCNT confines gemcitabine inside its cavity, while the outer surface is wrapped by chitosan in which one end is linked to the EGF. The results showed that in the EGF/30CS/SWCNT/Gemzar DDS the 30CS chain was not long enough to wrap around the SWCNT, and consequently the EGF was located so close to the tube as to potentially cause steric inhibition of the binding of EGF to its receptor (EGFR), which is highly expressed on the surface of cancer cells. On the other hand, this phenomenon is not observed in the EGF/60CS/SWCNT/Gemzar DDS in which the 60CS was found to completely wrap over the CNT outer surface using only 50 chitosan units. Although an increase in the temperature is likely to influence the overall DDS structure, and especially the orbit of helical chitosan on the SWCNT and the EGF conformation, gemcitabine is still encapsulated inside the tube.

4. Monte Carlo Simulation for Isotropic–Nematic Phase Transition of Infinitely Thin Liquid Crystal Molecules

We are also interested in isotropic–nematic phase transition of liquid crystal molecules. We gave a criterion to test a non-biaxial behavior of infinitely thin hard platelets based upon the components of three order parameter tensors. We investigated the nematic behavior of monodisperse infinitely thin rectangular hard platelet systems by this criterion. Starting with a square platelet system, and we compared it with rectangular platelet systems of various aspect ratios. For each system, we performed equilibration runs by using isobaric Monte Carlo simulations. Each system did not show a biaxial nematic behavior but a uniaxial nematic one, despite of the shape anisotropy of those platelets. The relationship between effective diameters by simulations and theoretical effective diameters of these systems was also determined.

Reference

- 1) H. Okumura, *Proteins: Struct., Funct., Bioinf.* **80**, 2397–2416 (2012).

Ultimate Quantum Measurements for Quantum Dynamics

Department of Theoretical and Computational Molecular Science
Division of Theoretical and Computational Molecular Science



SHIKANO, Yutaka
NAKANE, Junko

Research Associate Professor (Feb., 2012–)
Secretary

Due to great development on experimental technologies, it is possible to capture quantum dynamics in some physical and chemical systems. On the other hand, all experiments are in principle open and dissipative systems. Up to now, the well-explained experiments are approximated to the equilibrium situation. However, by recent technological development, some experiments reach to a transition from equilibrium to non-equilibrium situations. While there are the well-known tools on the non-equilibrium situations; the linear response theory and the Keldysh Green function method, this analysis cannot basically catch dynamical situations. Our goal is to construct the time-resolved theoretical models included the non-equilibrium situations. However, the quantum measurement theory is needed on measuring quantum dynamics, especially considering the measurement backaction. Our current activities are to resolve how sensitive (quantum) measurement can we carry out in principle, to build up some toy models on quantum dynamic, and to explain photoluminescence phenomenon in nitrogen vacancy center in diamond.

1. Quantum Measurement Sensitivity without Squeezing Technique¹⁾

As alluded before, our aim is to capture quantum dynamical phenomena. Capturing some phenomena needs to carry out the measurement. The conventional quantum measurement technique has huge measurement backaction. The measurement backaction prevents us chasing quantum dynamics like the classical trajectory. On the other hand, reducing the measurement backaction needs the tiny coupling between the target and probe quantum systems. However, under this situa-

tion, the signal in the probe system is also tiny small, that is, it is difficult to capture information. To resolve this problem, the squeezing technique was proposed and was experimentally implemented. However, this technique is practically difficult to be implemented. Our proposal is to use the weak measurement initiated by Aharonov, Albert, and Vaidman without squeezing technique. The profound meaning and interpretation of the weak measurement is seen in the review paper.²⁾ The key of this method is to take the post-selection of the target system. Due to this effect, tiny probe signal can be amplified. In the original proposal by Aharonov, Albert, and Vaidman, the amplification factor is infinite by the approximation method. However, the effect measurement backaction is simultaneously amplified. When the probe state is Gaussian to be used in the original proposal, we have analytically shown the upper bound of the amplification factor. We have analytically derived the probe state to maximally amplify the signal by the variational method.¹⁾ By this optimal probe state, the amplification factor has no upper bound. Our result tells us the infinitely amplified signal under the known coupling between the target and the probe. However, this result is ignored to consider the noise. We will extend our result to the signal-to-noise ratio optimization. Also, we are collaborating with the experiments to amplify the signal and consider the applications; the gravitational wave detector.

2. Discrete Time Quantum Walk as Quantum Dynamical Simulator³⁾

The discrete time quantum walk is defined as a quantum mechanical analogue of the classical random walk but is not the quantization of the classical random walk. This mathemati-

cal description is very simple but leads to many quantum dynamical phenomena. This is a toy model to better understand the quantum dynamics. Also, this has recently been various experimental demonstrations in the ultracold atoms in the optical lattice, trapped ions, and optical systems. We have analytically shown that the one- and two-dimensional discrete time quantum walks can be taken as the quantum dynamical simulator,³⁾ which concept is to emulate some classes of the differential equations, for example, the Dirac equation. Our approximation is used from the discrete lattice to continuous line for the large time steps of the discrete time quantum walk. This mathematical treatment is so powerful like the relationship between the cellular automaton and the integrable system.

3. Photoluminescence Phenomenon from Solid-State System⁴⁾

A method to measure some physical properties by light is widely used in physical, chemical, and biological systems. Therefore, laser science has been developed along with our demands from science and technology. A single photon source is expected as the low power laser source and the quantum communication tool. A nitrogen vacancy center in diamond and a quantum dot in a semiconductor system are the promising candidate of the single photon source. Especially, a nitrogen vacancy center in diamond has been attracted since this is run at room temperature. For an application as the highly controlled photon source, the photoluminescence process in the nitrogen vacancy center in diamond needs to be well understood. This system has the $S = 1$ electronic spin with the hyperfine structure 2.87 GHz. Furthermore, inserting a magnetic field, the different magnetic states are separated due to the Zeeman shift. Since this electronic spin is highly

localized, the local magnetic field evaluation is needed. We have shown the method to evaluate the local magnetic field from the conventional confocal microscopy.⁴⁾ Also, the nitrogen vacancy center in diamond is a candidate of the quantum memory. Since a lifetime of the nuclear spin of a ^{13}C atom nearly located in the nitrogen vacancy spot is long (\sim sec order), the perfect quantum state transfer is needed. However, it is difficult to evaluate the location of the ^{13}C atom. On the other word, it is difficult to evaluate the coupling constant between the electronic spin of the nitrogen vacancy center and the nuclear spin of the ^{13}C atom. We have proposed the simple scheme to evaluate the coupling constant between the two spins system under the dissipative situation.⁵⁾ As the next step, we will study the photoluminescence process from the nitrogen vacancy center in diamond.

As the current activities of our laboratory, we are studying the photoluminescence processes of the quantum dots and the exciton-polariton Bose-Einstein condensations in the two dimensional electronic gas of the semiconductor. These materials are expected to be used as the classical optical devices; the optical switching, collaborated with the various experimentalists.

References

- 1) Y. Susa, Y. Shikano and A. Hosoya, *Phys. Rev. A* **85**, 052110 (2012).
- 2) Y. Shikano, *Time in Weak Value and Discrete Time Quantum Walk*, LAP Lambert; Germany (2012).
- 3) K. Chisaki, N. Konno, E. Segawa and Y. Shikano, *Quant. Infor. Comput.* **11**, 0741–0760 (2011).
- 4) S. Kagami, Y. Shikano and K. Asahi, *Phys. E* **43**, 761–765 (2011).
- 5) Y. Shikano and S. Tanaka, *Europhys. Lett.* **96**, 40002 (2011).

Theoretical Studies of Chemical Dynamics in Condensed and Biomolecular Systems

Department of Theoretical and Computational Molecular Science
Division of Theoretical and Computational Molecular Science



ISHIZAKI, Akihito
YAMADA, Mariko

Research Associate Professor (March, 2012–)
Secretary

Photosynthesis provides the energy source for essentially all living things on Earth, and its functionality has been one of the most fascinating mysteries of life. Photosynthetic conversion of the energy of sunlight into its chemical form suitable for cellular processes involves a variety of physicochemical mechanisms. The conversion starts with the absorption of a photon of sunlight by one of the light-harvesting pigments, followed by transfer of electronic excitation energy to the reaction center, where charge separation is initiated. At low light intensities, surprisingly, the quantum efficiency of the transfer is near unity. A longstanding question in photosynthesis has been the following: *How does light harvesting deliver such high efficiency in the presence of disordered and fluctuating dissipative environments? Why does not energy get lost?* At high light intensities, on the other hand, the reaction center is protected by regulation mechanisms that lead to quenching of excess excitation energy in light harvesting proteins. The precise mechanisms of these initial steps of photosynthesis are not yet fully elucidated from the standpoint of molecular science.

1. Electronic Excitation Transfer Dynamics in Light Harvesting Systems

Recently, the technique of two-dimensional electronic spectroscopy has been applied to explore photosynthetic light harvesting complexes. The observation of long-lived quantum superposition or coherence between eigenstates of electronic excitations (excitons) in a pigment-protein complex stimulated a huge burst of activity among experimentalists and theorists. Much of the interest arose because the finding of electronic

quantum coherence is a “warm, wet, and noisy” biological system was considered very surprising. The initial experiments were carried out at 77 K, but more recent studies have detected coherence lasting at least 300 fs at physiological temperatures. These observations have led to the suggestion that electronic quantum coherence might play a role in achieving the remarkable efficiency of photosynthetic light harvesting. At the same time, the observations have raised questions regarding the role of the surrounding protein in protecting the coherence. In order to elucidate origins of the long-lived electronic coherence and its interplay with the protein environment, we have investigated appropriate theoretical frameworks and concepts with the use of statistical mechanics¹⁾ and in cooperation with experiment.²⁾

In particular, we have discussed significance of the finite timescale site-dependent reorganization dynamics of the protein environment surrounding (bacterio)chlorophyll molecules. The electronic coupling $\hbar J$ between pigments and the excitation-environment coupling characterized by the reorganization energy $\hbar\lambda$ are two fundamental interaction mechanisms determining the nature of electronic energy transfer (EET) in photosynthetic complexes. Ordinarily, photosynthetic EET is discussed only in terms of the mutual relation between magnitudes of the two couplings, as just described. However, the nature of EET also depends on the mutual relation between two timescales, the characteristic timescale of the environmental reorganization, τ (Figure 1), and the inverse of the electronic coupling, J^{-1} , that is the time the excitation needs to move from one pigment to another neglecting any additional perturbations. We showed that even in the region of reorganization energy much larger than that of a typical situation of photosynthetic light harvesting the sluggish reorganization

dynamics allows the excitation to stay above an energy barrier separating two local minima, which correspond to the two sites in the adiabatic potential surface, for a prolonged time (Figure 2). This is an essential origin of the experimentally observed long-lived electronic coherence.

Further, we showed this energy barrier is much small in comparison with the thermal energy $k_B T$ (almost activation-less) in the parameter regime corresponding to natural light harvesting systems. It can be considered that natural photosynthetic light harvesting systems avoid local trapping of electronic excitations, which yields a situation that electronic excitation energy gets lost in the presence of disordered and fluctuating dissipative environments. By extending this argument, we are now tackling the above questions regarding the remarkable quantum efficiency and smart regulation mechanism that photosynthetic light harvesting systems exhibit.

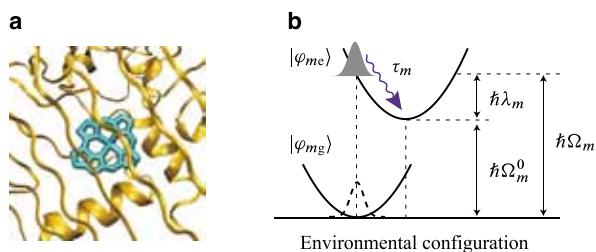


Figure 1. Schematic illustration of the m th pigment embedded in a protein (a) and the electronic ground and excited states of the m th pigment, $|\varphi_{mg}\rangle$ and $|\varphi_{me}\rangle$, affected by nuclear motion of the protein environment (b). After electronic excitation in accordance with the vertical Franck-Condon transition, reorganization takes place from the equilibrium nuclear configuration with respect to the electronic ground state $|\varphi_{mg}\rangle$ to the actual equilibrium configuration in the excited state $|\varphi_{me}\rangle$ with dissipation of the reorganization energy, $\hbar\lambda_m$. This reorganization of the protein environment proceeds on a characteristic timescale, τ_m .

Award

ISHIZAKI, Akihito; Short-term Fellowship at Wissenschaftskolleg zu Berlin, 2012/2013.

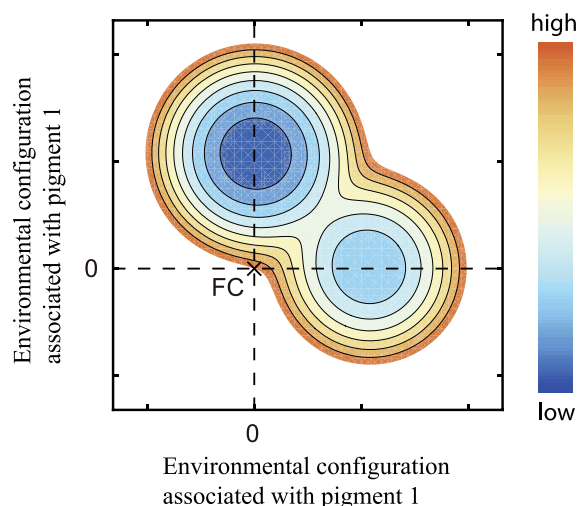


Figure 2. Schematic illustration of adiabatic excitonic potential surface of coupled two pigments. The point of origin corresponds to the Franck-Condon state. The energy of the point is higher than the barrier between the minima; therefore, we find that the electronic excited state is delocalized just after the excitation. As time increases, the dissipation of reorganization energy proceeds and the excitation will fall off into one of the minima and become localized. Namely, sluggish dissipation of reorganization energy increases the time an electronic excitation stays above an energy barrier separating pigments and thus prolongs delocalization over the pigments.

References

- 1) A. Ishizaki and G. R. Fleming, *Annu. Rev. Condens. Matter Phys.* **3**, 333–361 (2012).
- 2) G. S. Schlau-Cohen, A. Ishizaki, T. R. Calhoun, N. S. Ginsberg, M. Ballottari, R. Bassi and G. R. Fleming, *Nat. Chem.* **4**, 389–395 (2012).
- 3) Y.-C. Cheng and A. Ishizaki, *J. Chem. Phys.* (invited), to appear.

Theory and Computation of Reactions and Properties in Solutions and Liquids

Department of Theoretical and Computational Molecular Science
Division of Computational Molecular Science



ISHIDA, Tateki

Assistant Professor

We focus on the projects both on ultrafast photoinduced electron energy transfer in the excited state in solution and on ionic liquids (ILs). The project on photoinduced electron energy transfer processes in the excited state in solution focuses on the development of a theoretical method to describe electron energy transfer including solvent motion and dynamics with the theoretical treatment we have developed. On the other hand, ILs' projects concentrate the study of specific interionic dynamics in ILs and the investigation of a new perspective on the physically and chemically unique characteristics of ILs.

1. The Theoretical Study of Photoinduced Electron Energy Transfer Processes in the Excited State in Solution

We have developed a procedure for describing the time-dependent evolution of the electronic structure of a solute molecule in solution, coupling an electronic structure theory with solvent motion in the formalism of an interaction site model. We extend this prescription for studying electron energy transfer processes in the excited state in solution. It is indicated that the coupling between solvation dynamics and a fast intramolecular electron energy transfer is likely to play an important role in the emergence of photoinduced unique functionalities in biochemical and metal complex systems.

2. The Unique Physical and Chemical Properties of Ionic Liquids through Interionic Interactions: Theoretical Investigation with Molecular Dynamics Simulations¹⁾

Ionic liquids (ILs) have been found to possess a wide potential variety of interesting physical and chemical properties. We consider the unique properties of ILs which owe to the specific interionic interaction between ionic species. In particular, we study the importance of both the cross-correlation between cation and anion species, and the effect of

polarization in ILs. On the basis of recent theoretical studies on ILs employing molecular dynamics simulations, how the collective dynamics through interionic interactions cause the unique physical and chemical properties of ILs and how electronic polarizability effects modify interionic dynamics have been investigated. Those include the investigation of the contribution of ionic motions with velocity cross-correlation functions and the study of many-body polarization effects on the cage effect in ILs.

3. Investigations of New Perspectives on the Characteristics of Ionic Liquids: Microscopic Aspects in Dicationic Ionic Liquids²⁾

The interionic vibrations in imidazolium-based dicationic ionic liquids (ILs) containing the bis(trifluoromethylsulfonyl)-amide ($[\text{NTf}_2]^-$) counteranion were investigated using femto-second optical-heterodyne-detected Raman-induced Kerr effect spectroscopy. The microscopic nature of the dicationic ILs ($[\text{C}_n(\text{MIm})_2][\text{NTf}_2]_2$, where $n = 6, 10,$ and 12 ; MIm = *N*-methylimidazolium) was compared with that of the corresponding monocationic ILs ($[\text{C}_n\text{MIm}][\text{NTf}_2]$, where $n = 3, 5,$ and 6) used as reference samples. Low-frequency Kerr spectra within the frequency range $0\text{--}200\text{ cm}^{-1}$ of the ILs revealed that the spectral profile of the dicationic ILs as well as that of the corresponding monocationic ILs is bimodal. The distinguished line-shape of the low-frequency Kerr spectrum of $[\text{C}_3\text{MIm}][\text{NTf}_2]$ from the other ILs can be accounted for by the homogeneous nature in the microstructure of the IL, but the other ILs indicate microsegregation structures due to the longer nonpolar alkylene linker or alkyl group in the cations.

References

- 1) T. Ishida, in *Handbook of Ionic Liquids: Properties, Applications and Hazards*, J. Mun and H. Sim, Eds., Nova Science Publishers Inc.; Hauppauge, NY, pp. 395–417 (2012).
- 2) H. Shirota and T. Ishida, *J. Phys. Chem. B* **115**, 10860–10870 (2011).

Visiting Professors



Visiting Associate Professor
HASEGAWA, Jun-ya (*from Kyoto University*)

Quantum Chemistry for the Excited States of Functional Molecules in Proteins and Solutions

Molecular interactions between chromophore and environment are the essential to furnish a protein with the photo-functionality. I am interested in the machinery of the photo-functions such as photosynthesis, vision, and bioluminescence. To understand the mechanism and to develop chemical concept behind the photo-functions, we develop electronic structure theories for excited state, analytical method for excitation-energy transfer pathway, and a hybrid quantum-mechanics/molecular mechanics method. In recent studies, we have clarified color-tuning mechanism of photo-functional proteins and excitation transfer mechanism of bridge-mediated donor-acceptor systems. We are also interested in developing a configuration interaction picture for the solvatochromic response of the molecular environment.



Visiting Associate Professor
ANDO, Koji (*from Kyoto University*)

Quantum Transfer Processes in Chemical and Biological Systems

At the core of chemistry and biochemistry are reduction-oxidation and acid-base reactions, whose elementary processes are electron and proton transfers. Our research group has been working on theoretical and computational modeling of these inherently quantum dynamical processes. One recent achievement is a development of electron transfer (ET) pathway analysis method with use of fragment molecular orbital calculations, by which the ETs in a bacterial photosynthetic reaction center have been studied. Another is a development of nuclear wave packet molecular dynamics simulation method and its applications to hydrogen-bond exchange dynamics in water. It has been also discovered that the latter can be extended to electron wave packet simulations by exploiting the non-orthogonal valence-bond theory, which anticipates a non-Born-Oppenheimer electron-nuclear dynamical treatment.



Visiting Associate Professor
MORISHITA, Tetsuya (*from AIST*)

First-Principles Molecular-Dynamics Simulations of Liquids and Glassy Materials

I have been interested in structural and dynamical properties of non-crystalline materials including nanoscale materials. In 2011, I have found that liquid silicon exhibits compressed exponential relaxation over a wide temperature range including the supercooled regime, in contrast to water and other glass-forming liquids, using first-principles molecular-dynamics simulations.

I have also developed a new method for free-energy calculation, Logarithmic Mean-Force Dynamics (LogMFD). This method was successfully applied to reconstruction of the free-energy profile of a dipeptide molecule, showing that LogMFD considerably outperforms conventional free-energy calculation methods such as thermodynamics integration.